The dynamic properties of intermediate filaments during organelle transport

Lynne Chang[1], Kari Barlan[2,*], Ying-Hao Chou[2,‡], Boris Grin[2,‡], Margot Lakonishok[2,*], Anna S. Serpinskaya[2,*], Dale K. Shumaker[2,3], Harald Herrmann[4], Vladimir I. Gelfand[2,§] and Robert D. Goldman[2]

[1]Department of Microbiology and Molecular Genetics, Harvard Medical School, Harvard University, Boston, MA 02115, USA
[2]Department of Cell and Molecular Biology, Feinberg School of Medicine, Northwestern University, Chicago, IL 60611, USA
[3]Department of Urology, Feinberg School of Medicine, Northwestern University, Chicago, IL 60611, USA
[4]Division of Molecular Genetics, German Cancer Research Center (DKFZ), Im Neuenheimer Feld 580, D-69120 Heidelberg, Germany
*,‡The authors from the laboratory of Vladimir I. Gelfand (indicated by *) and the authors from the laboratory of Robert D. Goldman (indicated by ‡) contributed equally to this work
§Author for correspondence (vgelfand@northwestern.edu)

Accepted 21 May 2009
Journal of Cell Science 122, 2914-2923 Published by The Company of Biologists 2009
doi:10.1242/jcs.046789

Summary

Intermediate filament (IF) dynamics during organelle transport and their role in organelle movement were studied using *Xenopus laevis* melanophores. In these cells, pigment granules (melanosomes) move along microtubules and microfilaments, toward and away from the cell periphery in response to α-melanocyte stimulating hormone (α-MSH) and melatonin, respectively. In this study we show that melanophores possess a complex network of vimentin IFs which interact with melanosomes. IFs form an intricate, honeycomb-like network that form cages surrounding individual and small clusters of melanosomes, both when they are aggregated and dispersed. Purified melanosome preparations contain a substantial amount of vimentin, suggesting that melanosomes bind to IFs. Analyses of individual melanosome movements in cells with disrupted IF networks show increased movement of granules in both anterograde and retrograde directions, further supporting the notion of a melanosome-IF interaction. Live imaging reveals that IFs, in turn, become highly flexible as melanosomes disperse in response to α-MSH. During the height of dispersion there is a marked increase in the rate of fluorescence recovery after photobleaching of GFP-vimentin IFs and an increase in vimentin solubility. These results reveal a dynamic interaction between membrane bound pigment granules and IFs and suggest a role for IFs as modulators of granule movement.

Supplementary material available online at
http://jcs.biologists.org/cgi/content/full/122/16/2914/DC1

Key words: Intermediate filament, Melanosome, Transport, Vimentin

Introduction

Cytoskeletal intermediate filament (IF) proteins are encoded by a family of ~70 genes (Zimek et al., 2003). These proteins, either singularly, or in cell-type-specific combinations, form filaments with a diameter of ~10 nm. IFs have a well-established function as the major mechanical integrators of cells and tissues. This is mainly attributable to their unique viscoelastic properties that render them more resistant to deformation under mechanical stress (Janmey et al., 1998; Kreplak et al., 2005; Helmke et al., 2001; Helmke et al., 2000; Sivaramakrishnan et al., 2008). In addition to their unusual viscoelasticity, IFs also exhibit highly dynamic properties in vivo (Chang and Goldman, 2004). These properties are at least in part due to interactions between IFs and the other cytoskeletal systems, microtubules (MTs) and microfilaments (MFs). The various structural forms of IFs, including IF-precursor particles, short filaments (squiggles), and long filaments, move at varying speeds along MTs and MFs, utilizing molecular motors such as conventional kinesin, cytoplasmic dynein and myosin V (Helfand et al., 2004; Rao et al., 2002). These various IF structures appear to be interconvertible. There is evidence that these interconversions are regulated by kinase-phosphatase equilibria, which are probably responsible for the rapid reorganization of IFs that takes place in response to various cellular signals (Eriksson et al., 2004; Chang and Goldman, 2004).

Based on their interactions with MTs, MFs and molecular motors (see Helfand et al., 2004), it is not surprising that IFs also appear to be involved in the distribution of membrane-bound organelles. Although the transport of membranous organelles is mainly mediated by molecular motors and their respective cytoskeletal tracks, MTs and MFs, their proper positioning in the cytoplasm frequently appears to involve interactions with IFs (Styers et al., 2005). For example, the distribution of mitochondria is closely associated with the organization of vimentin IFs and neurofilaments (NFs) (Mose-Larsen et al., 1982; Collier et al., 1993). The interaction between NFs and mitochondria appears to be regulated by the phosphorylation state of the NF side arms and the mitochondrial membrane potential in vitro (Wagner et al., 2003).

The distribution of the Golgi complex and late endosomal/lysosomal complexes also appears to be modulated by interactions with vimentin IFs. The Golgi interactions with IFs appear to be mediated through a peripherally associated Golgi protein, formiminotransferase cyclodeaminase (Gao and Sztul, 2001; Gao et al., 2002), whereas the association with the endo-lysosomal sorting machinery appears to involve the adaptor complex AP3 (Styers et al., 2004). Interestingly, the AP3 complex also participates in cargo selection for organelles such as melanosomes (pigment granules) and the dense granules of blood platelets (Kantheti et al., 1998). Although it is well established that vimentin IF are major cytoskeletal components of lower vertebrate melanophores (Gyoeva et al., 1987), little is known about their organization, structure and function with respect to the melanosomes in these cells. The most significant evidence that melanosomes and vimentin IFs interact

comes from studies demonstrating that the processivity of both anterograde and retrograde movements increases significantly when the normally extended vimentin IF network in melanophores is disrupted (Kural et al., 2007). This increase in uninterrupted runs occurred in both plus- and minus-end-directed movements. Furthermore, in the absence of IFs, myosin V-mediated movements had shorter rise-times, suggesting that IFs physically impede melanosome movement by increasing viscous drag (Kural et al., 2007).

In the present work, we have analyzed the dynamics of vimentin IFs and their interaction with melanosomes during transport in *Xenopus laev*is melanophores. In these cells, hundreds of melanosomes move toward the cell periphery in response to an increase in the concentration of cAMP triggered by α-melanocyte-stimulating hormone (MSH), whereas melatonin-induced decrease in cAMP concentration causes melanosome aggregation near the cell center. The ability to trigger the rapid and simultaneous movement of organelles by well-defined chemical signals makes melanophores an ideal model system for studying organelle transport. Microscopic and biochemical analyses demonstrate that vimentin IFs form cage-like structures surrounding individual and small clusters of melanosomes. In this fashion, IF form an intricate honeycomb-like network, which is independent of MT networks. We also show that vimentin IF dynamics and solubility change rapidly during α-MSH and melatonin treatment, potentially allowing for more efficient melanosome movement. Based on morphological grounds, live-cell imaging and biochemical analyses, we propose a role for IF in the regulation of the coordinated transport and positioning of melanosomes to targeted sites within cells.

Results

Xenopus melanophores contain a complex network of vimentin intermediate filaments surrounding melanosomes

Immunofluorescence reveals a close relationship between vimentin, the major IF protein expressed in *Xenopus laev*is melanophores, and melanosomes. Vimentin filaments form an intricate network extending from the perinuclear region to the cell periphery (Fig. 1B). Although a portion of the IF network appears to overlap with other cytoskeletal networks such as microtubules (MTs), upon closer inspection the honeycomb pattern of IF distribution is quite distinct from the relatively sparse, radial distribution of MTs (Fig. 1E,F,I). Individual and small clusters of melanosomes appear to be enmeshed in the vimentin network. Indeed, most melanosomes appear to be surrounded by cage-like structures of IFs (Fig. 1D,E,G). This close association can be seen in cells containing either aggregated or dispersed melanosomes (see supplementary material Fig. S1 for cells containing aggregated melanosomes). The relationship between IFs and melanosomes was also examined at higher resolution by platinum replica electron microscopy. The processing of cells for this ultrastructural analysis involved a method that preserves IFs while removing MTs and MFs (Svitkina et al., 1995; Helfand et al., 2002; see Materials and Methods). This technique revealed that the pattern of IF distribution seen by indirect immunofluorescence was largely retained by the EM preparation and that each melanosome was closely associated with large numbers of IFs in both the aggregated and dispersed states (Fig. 1J-L).

We also carried out cell fractionation studies to determine whether there was a biochemical connection between melanosomes and IFs. To this end, we purified melanosomes through 80% Percoll density gradients (Rogers et al., 1997). Since melanosomes contain a very high concentration of melanin, they are efficiently separated

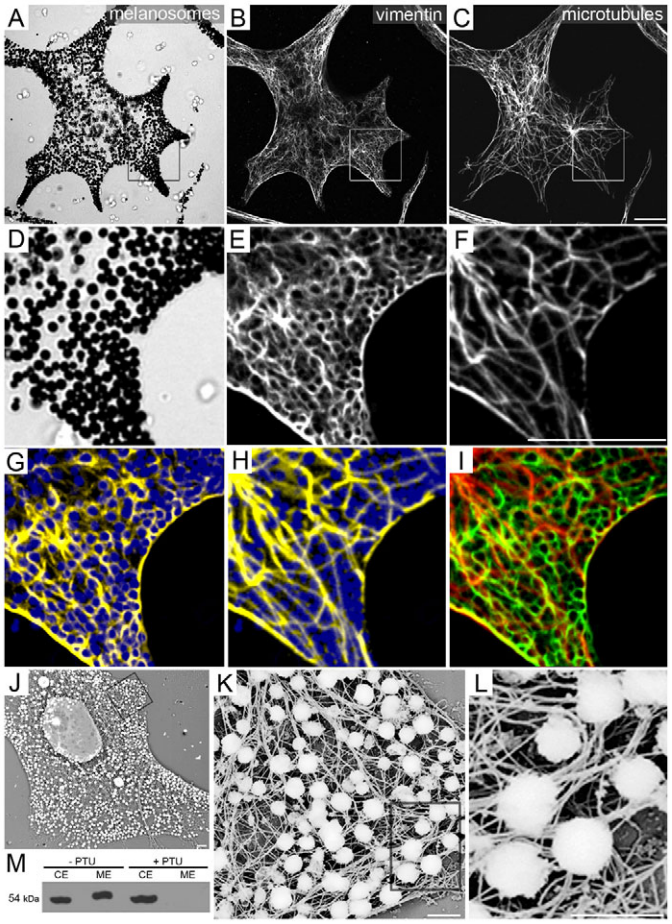

Fig. 1. Microscopic and biochemical evidence for vimentin association with melanosomes in *Xenopus* melanophores. (A-C) Immunofluorescence preparation of melanophores reveals a dense network of vimentin filaments (B) that permeate the cytoplasm. Microtubules form a sparse, radial network (C). Scale bar: 5 μm. (D-F) Higher magnification images of boxed regions in A-C show melanosomes (D) surrounded by a dense network of vimentin filaments (E). Scale bar: 5 μm. (G-I) Pseudo-colored overlays of D-F. Vimentin fibers (yellow) wrap around individual and clusters of melanosomes (blue; G). This encaging is not observed between microtubules (yellow) and melanosomes (blue; H). An overlay of vimentin (green) and microtubules (red) is shown in I. (J-L) Melanophores were processed for platinum replica electron microscopy using a technique that preserves intermediate filaments and dissolves microtubules (MTs) and actin filaments (MFs) (Svitkina et al., 1995) (see Materials and Methods). Melanosomes appear to remain closely associated with vimentin filaments in the absence of MTs and MFs. K and L are higher magnification views of J. Scale bars: (J) 2 μm; (K,L) 1 μm. (M) Western blot analysis of purified melanosomes using an antibody specific for vertebrate vimentin shows co-purification of vimentin with the granules in wild-type cells (–PTU; CE, total cell extract; ME, melanosome extract). Vimentin co-purifies with granules isolated from melanophores treated with either melatonin or α-melanocyte stimulating hormone (α-MSH; unpublished data). In PTU-treated cells that lack melanosomes, vimentin is not present in the pellet (+PTU).

from other membranous organelles which do not enter 80% Percoll. Furthermore, soluble proteins such as tubulin are excluded by the Percoll step (Rogers et al., 1997) (and unpublished data). We have previously shown that cytoplasmic dynein, kinesin II (Rogers et al., 1997) and myosin V (Rogers and Gelfand, 1998) co-purify with melanosomes through these Percoll gradients. These earlier studies also showed an enrichment of an ~55 kDa band in the purified melanosome fraction, which did not correspond to tubulin (Rogers

et al., 1997) (and unpublished data). Analysis of the melanosome preparations using western blotting with anti-vimentin antibodies shows that a significant amount of vimentin co-purifies with melanosomes (Fig. 1M; –PTU lanes). This co-purification also appears to be independent of the position of the granules (aggregated or dispersed; unpublished data). To demonstrate that the presence of vimentin in the melanosome fraction is the result of IF-melanosome binding, we used melanosome-free cells as a source of material for purification. Melanosome-free melanophores were prepared by growing cells in the presence of 1-phenyl 2-thiourea (PTU), an inhibitor of tyrosinase, the key enzyme involved in melanin biosynthesis (Gross et al., 2002). Melanophores grown in PTU lose their melanosomes, but otherwise grow normally and retain all components of the cytoskeleton including vimentin IFs (supplementary material Fig. S2; Fig. 3G-I). Extracts of PTU-treated cells were prepared following the same treatment as for Percoll gradient purification of cells with melanosomes. The resulting pellet contained no vimentin (Fig. 1M; +PTU lanes). This demonstrates that vimentin only pellets through Percoll because it is bound to melanosomes.

In order to determine whether the observed associations between vimentin and melanosomes were organelle specific, we co-imaged vimentin (antibody staining), melanosomes (bright-field illumination) and lysosomes labeled with fluorescent LysoTracker Red. In contrast to the observed encaging of individual melanosomes by vimentin filaments (Fig. 1G, Fig. 2D), individual lysosomes were rarely surrounded by IFs (Fig. 2E,F), suggesting specificity in melanosome-IF associations.

Since it has been shown that melanosomes move primarily along microtubule (MT) tracks during their dispersion we investigated whether these cytoskeletal components were necessary to maintain their positions following treatment with α-MSH. Double label immunofluorescence preparations revealed that vimentin IFs and MTs are not closely associated with each other in the dispersed state (Fig. 1I). Interestingly, the disruption of MTs by nocodazole, which normally induces the retraction of vimentin IFs into a juxtanuclear cap in cultured fibroblasts (Goldman, 1971), did not affect either the distribution of the IF networks or the dispersed melanosomes (Fig. 3A-F). Similar results were obtained in cells in which the melanosomes were not dispersed (unpublished data). Furthermore, vimentin IF networks in melanosome-free cells, obtained by PTU treatment, were not affected by nocodazole treatment and remained extended throughout the cytoplasm (Fig. 3G-L), suggesting that the MT-independent distribution of vimentin IFs in melanophores is not mediated by attachment to melanosomes.

More melanosomes move in the absence of a vimentin network

The close association we observed, both structurally and biochemically, between vimentin IFs and melanosomes suggests a tethering or anchoring role for vimentin IFs. To test this possibility we used a GFP-tagged dominant negative construct [GFP-vimentin(1-138)] that encodes the non-α-helical head domain (residues 1-102) and the first 36 amino acids of the highly

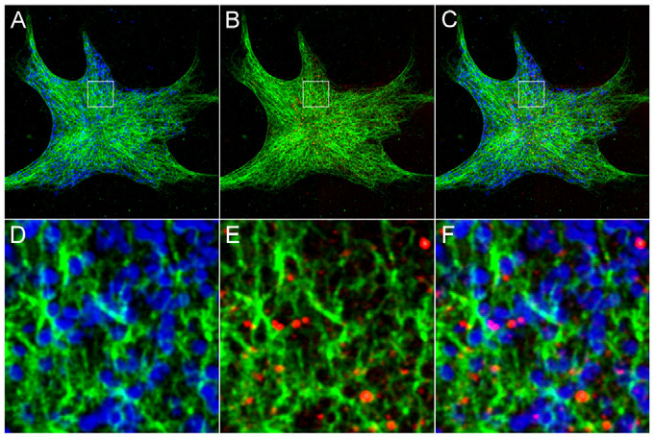

Fig. 2. Lysosomes are not closely associated with vimentin IFs. Melanophores were incubated with LysoTracker Red for 1 hour to visualize lysosomes, followed by processing for immunofluorescence to detect vimentin. Melanosomes were imaged using bright-field illumination and the image was inverted and given a blue hue in Photoshop. A-C show a low magnification, double (A,B) and triple (C) overlay images of vimentin (green), melanosomes (blue) and fluorescently labeled lysosomes (red). (D-F) Higher magnification images of the boxed regions in A-C show very few lysosomes that are closely associated with vimentin IFs.

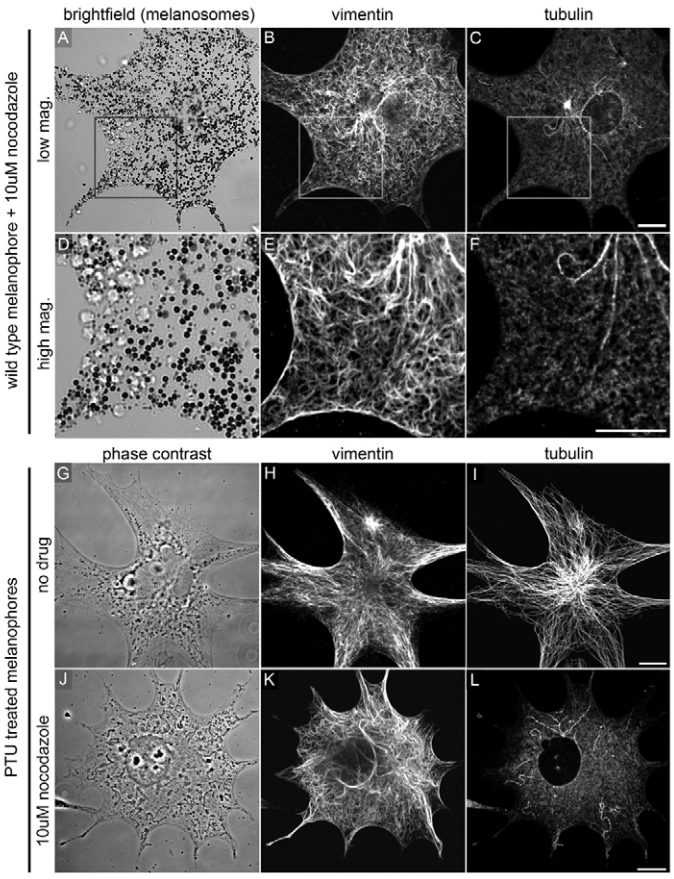

Fig. 3. Vimentin IFs association with melanosomes is independent of microtubules. (A-C) The distribution of vimentin IFs is not affected by nocodazole-induced depolymerization of MTs. The IF network remains fully extended and densely distributed throughout the cytoplasm. See Fig. 1A-F for comparison. Scale bar: 5 μm. (D-F) Higher magnification images of the boxed regions in A-C show vimentin filaments surrounding melanosomes in the absence of MTs. Scale bar: 5 μm. (G-I) The vimentin IF network is similarly distributed as an extended network in PTU-treated melanophores that lack melanosomes. Scale bar: 5 μm. (J-L) Nocodazole treatment of these cells does not appear to cause reorganization of the vimentin IF network, demonstrating that vimentin IF distribution is not a result of melanosomes anchoring IFs. Scale bar: 5 μm.

conserved α-helical domain (coil 1A) of vimentin. When this vimentin(1-138) segment is expressed in *Xenopus* melanophores as a GFP fusion protein, it functions as a dominant negative disruptor of vimentin IF assembly (Kural et al., 2007). We have also shown previously that mimetic peptides corresponding to the coil 1A domain are potent disruptors of endogenous vimentin IFs both in vivo and in vitro (Goldman et al., 1996). Disruption of the endogenous vimentin IF network by GFP-vimentin(1-138) was confirmed by immunostaining cells 48 hours post-transfection with a vimentin antibody (Fig. 4B). The mutant protein and the endogenous vimentin were co-aggregated near the nucleus and the peripheral cytoplasm was nearly devoid of filamentous vimentin. Microtubules and microfilament bundles appeared normal in these cells (Fig. 4D,F, respectively). As a control, cells were transfected with a GFP-tagged full-length *Xenopus* vimentin (GFP-vimentin) and immunostained for MTs and MFs (Fig. 4C,E, respectively).

As vimentin IFs form a dense network in the cytoplasm of melanophores, we sought to understand the contribution of IFs to melanosome motility. Analysis of melanosome behavior in cells expressing GFP-vimentin(1-138) showed that the number of moving melanosomes as well as their speed increased in both retrograde (–) and anterograde (+) directions when compared with cells containing an intact IF network (Fig. 5A,B). Lysosomal movement was not affected by the absence of a vimentin network (Fig. 5C), further confirming the specificity of melanosome-vimentin interactions. Interestingly, despite the increase in the numbers of moving melanosomes and their speed, disruption of the vimentin IF network did not affect the end-states of melanosome transport: both GFP-vimentin(1-138)-transfected and control cells contained primarily dispersed melanosomes at 60 minutes after α-MSH

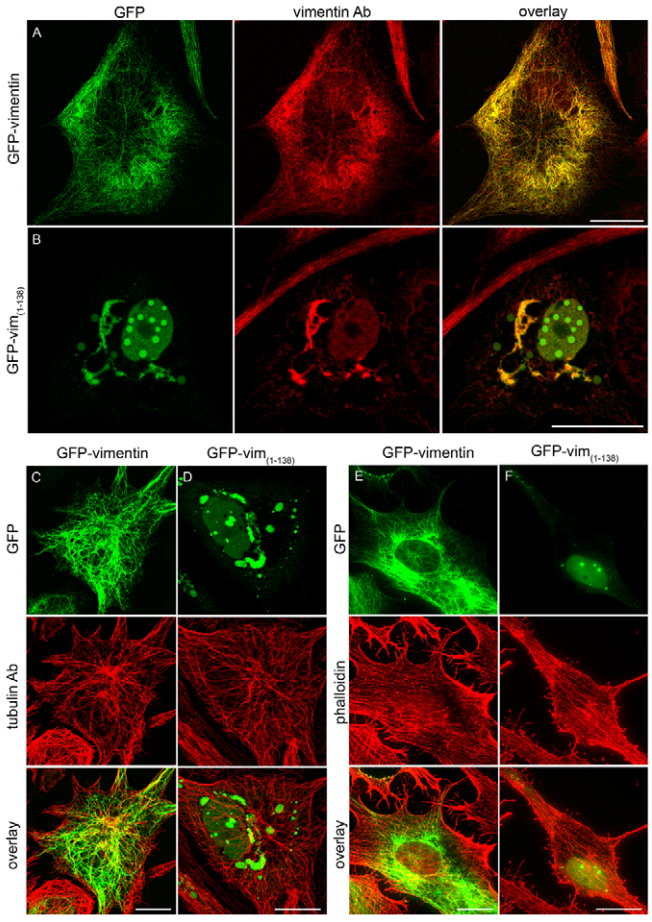

Fig. 4. GFP-vimentin incorporates into the endogenous vimentin IF network and a GFP-tagged truncated vimentin construct disrupts the endogenous network in *Xenopus* melanophores. (A) Cells were transfected with a GFP-tagged full-length *Xenopus* vimentin construct for 48 hours. The GFP-vimentin (shown in green) co-assembles with endogenous vimentin (visualized by antibody staining; shown in red). (B) Cells transfected for 48 hours with a dominant-negative construct containing the head and alpha-helical domain 1A of vimentin [GFP-vim(1-138)] have a disrupted endogenous network. The truncated vimentin forms aggregates in the nucleus and perinuclear area, and sequesters the endogenous vimentin away from the peripheral cytoplasm. The truncated vimentin was tagged with a C-terminal GFP (shown in green), and the endogenous network was visualized by immunostaining (shown in red). (C,D) Disruption of vimentin IFs does not affect the distribution of microtubules. Cells were transfected with either full-length GFP-vimentin (C; green) or GFP-vim(1-138) (D; green) for 48 hours and immunostained with a microtubule-specific antibody (red). (E,F) Disruption of vimentin IFs does not affect the distribution of actin filaments. Cells were transfected with either full-length GFP-vimentin (E; green) or GFP-vim(1-138) (F; green) for 48 hours. Actin filaments were visualized by phalloidin (red). Scale bars: 20 μm.

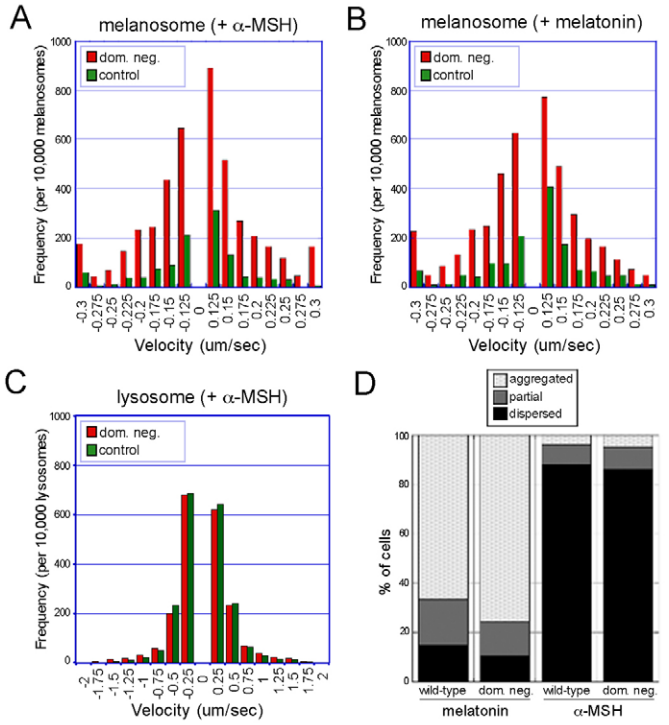

Fig. 5. Melanosomes move more in the absence of a vimentin IF network. (A,B) The number of moving melanosomes and their speed were elevated in both retrograde (–) and anterograde (+) directions in cells expressing the dominant negative vimentin construct, GFP-vim(1-138) (dom. neg.), when compared with control cells. These increases were evident during both dispersion by α-MSH treatment and melatonin-induced aggregation. (C) In contrast to melanosomes, lysosomal movement was not affected by the expression of GFP-vim(1-138) (dom. neg.) as compared with control cells. Lysosomes were tracked in cells treated with α-MSH to mirror the melanosome dispersion situation. Similar results were obtained in unstimulated cells (not shown). (D) Disruption of the vimentin IF network by overexpression of the dominant negative vimentin (dom. neg.), did not affect the end states of melanosomes in response to melatonin and α-MSH at 60 minutes after hormone treatment. Melanosomes were predominantly aggregated in both transfected and wild-type cells in response to melatonin and dispersed in both cell types in response to α-MSH.

treatment and contained predominantly aggregated melanosomes at 60 minutes after melatonin treatment (Fig. 5D).

Vimentin IFs undergo extreme shape changes during melanosome movement

The close association between vimentin IFs and melanosomes and the effects of the dominant-negative vimentin construct on melanosome transport suggest that the IF network is a formidable impediment to the rapid motility of melanosomes during both their anterograde and retrograde movements in response to α-MSH and melatonin, respectively. Therefore it was of interest to know how melanosomes manage to move through this dense and complex network of IFs during their dispersion and/or aggregation in response to stimuli such as α-MSH or melatonin. To address this, we carried out live-cell imaging analyses to determine whether there were changes in vimentin IF dynamics to accommodate granule dispersion. For these studies, GFP-vimentin was expressed in melanophores. Its incorporation into the endogenous network was confirmed by immunostaining with a vimentin antibody (Fig. 4A). GFP-vimentin-expressing cells were serum deprived for 2 hours, followed by treatment with melatonin to aggregate melanosomes. Subsequently the cultures were washed with serum-free medium and α-MSH was added to stimulate granule dispersion. Cells were imaged using a spinning disk confocal microscope with 5-second frame intervals (supplementary material Movie 1; Fig. 6). Before α-MSH addition, IFs exhibited minimal bending motions and translocations (unpublished data). By contrast, during granule dispersion, vimentin IFs underwent rapid shape changes, including extensive bending and straightening movements. For example, the time-lapse frames in Fig. 6B,C show a granule (pseudo-colored purple) moving towards the lower left field of view while a vimentin filament in the path bends and appears to yield to its movement. To study IF dynamics during melanosome aggregation, we treated cells with H-89, an inhibitor of cyclic AMP-dependent protein kinase (PKA) (Chijiwa et al., 1990). Melatonin could not be used for live-imaging of granule aggregation as light used during imaging activates melanopsin, stimulating adenylate cyclase and increasing the concentration of cAMP (Provencio et al., 1998). Therefore, for time-lapse imaging of aggregation, we used H-89, which inhibits the PKA pathway downstream of cAMP. Interestingly, in response to H-89 treatment vimentin IFs appeared to become more straight and rigid in the path of moving granules as they vacated the peripheral cytoplasm and aggregated near the nucleus (supplementary material Movie 2). IFs in the granule-rich region near the nucleus formed a honeycomb-like network surrounding individual and small clusters of granules (supplementary material Fig. S1), similar to the IF network surrounding granules in dispersed cells (Fig. 1E,G).

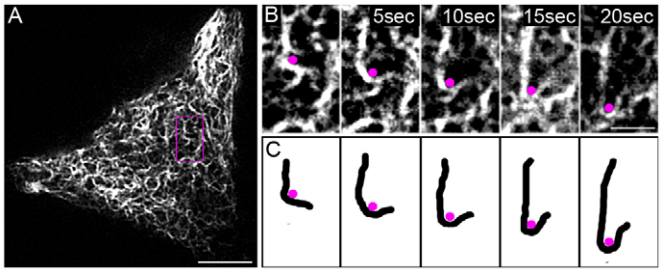

Fig. 6. Vimentin filaments undergo dramatic shape changes during melanosome movement. *Xenopus* melanophores expressing GFP-vimentin were used for live-imaging experiments. These cells were serum starved for 2 hours, followed by treatment with α-MSH to stimulate granule dispersion and then imaged using a spinning disk confocal microscope with 5-second frame intervals. (A) A low magnification image at time point 0 (scale bar: 5 μm). (B) Higher magnification, time-lapse frames show a granule, pseudo-colored purple, moving with the vimentin filament that bends and moves toward the lower left field of view (scale bar: 1 μm; also see supplementary material Movie 1). (C) A cartoon depiction of the relevant filament and granule from B, for easier visualization.

Hormone stimulation of melanosome movement elevates vimentin IF dynamics and solubility

The increased bending motions and apparent flexibility of vimentin IFs during melanosome dispersion raised the question of whether IF subunit turnover and exchange was increased. In order to test this possibility, fluorescence recovery after photobleaching (FRAP) analyses were performed on GFP-vimentin-expressing cells during melanosome dispersion and compared with cells after dispersion (Fig. 7A). At ~16 minutes after photobleaching, GFP-vimentin in dispersing cells had recovered ~72% of its fluorescence. In cells with fully dispersed pigment granules only ~22% recovery took place after the same time interval (Fig. 7B). The difference between the average $t_{1/2}$s of fluorescence recovery between cells actively dispersing melanosomes and cells with fully dispersed melanosomes was statistically significant (P=0.037; n=4 cells per treatment condition), suggesting that there was a larger pool of exchangeable vimentin subunits during active granule dispersion. FRAP data from cells undergoing granule aggregation was difficult to obtain even with H-89, as the prolonged illumination required for photobleaching and time-lapse imaging triggered dispersion of granules (not shown) (Daniolos et al., 1990). FRAP analysis of cells with aggregated granules (prior to α-MSH addition) could not be carried out because of similar technical difficulties.

Unlike the problems inherent in live-imaging and FRAP (see above) (Daniolos et al., 1990), biochemical analysis of cells undergoing granule aggregation was made possible by maintaining melatonin-treated cells in the dark with minimum exposure to light. Serum-starved melanophores were treated with either α-MSH or melatonin and then lysed at various time points during dispersion or aggregation of granules. The soluble and insoluble fractions were separated by centrifugation at 12,000 ***g*** for 10 minutes and then the relative amounts of vimentin in soluble and pelletable fractions were measured by quantitative western analysis (Goldman et al., 1996). Regardless of the type of hormone treatment, there was a transient increase in vimentin solubility following the induction of either type of movement, followed by a decrease to initial levels (Fig. 7C). Three independent experiments were carried out for each hormone treatment and all six yielded similar results [mean (± s.d.) values are shown in Fig. 7D). Both the increase (between time points 1 and 40 minutes for melatonin and 30 minutes for α-MSH) and decrease (between time points 40 or 30 minutes and 60 minutes) were statistically significant (P-values for the increase were 0.02 for melatonin and 0.0072 for α-MSH; P-values for the decrease were 0.018 for melatonin and 0.026 for α-MSH). Interestingly, this peak in vimentin solubility temporally coincides with the height of melanosome movement (be it dispersion or aggregation). Cessation of long-distance melanosome movement occurs around 60 minutes post hormone treatment, when vimentin solubility is low (Fig. 5D).

Since IF solubility is known to be regulated by protein phosphorylation (Eriksson et al., 2004), vimentin IFs in dispersing and aggregating melanophores were analyzed for changes in phosphorylation levels. Cells were labeled with [^{32}P]orthophosphate

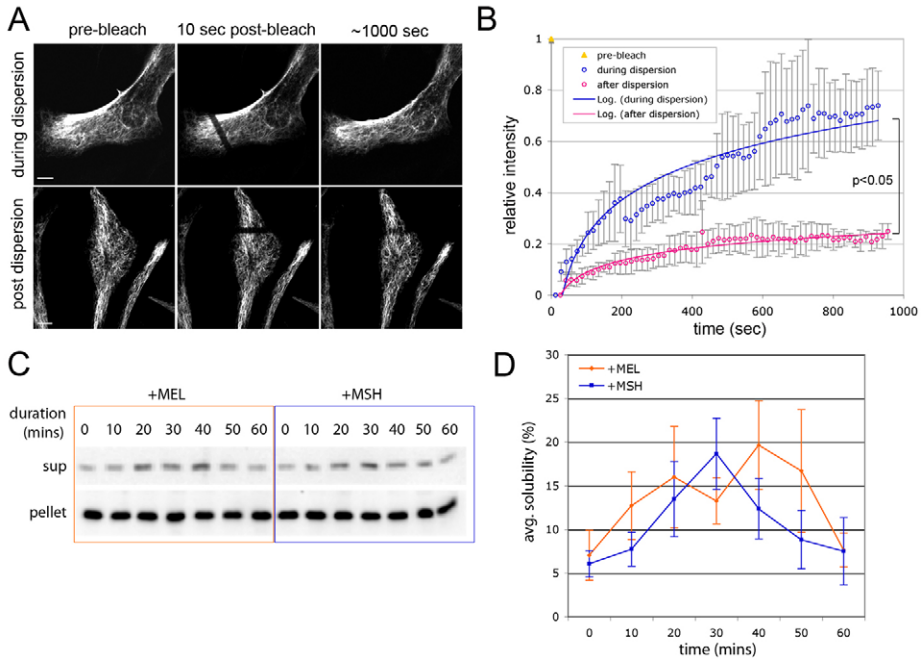

Fig. 7. There is a higher fraction of exchangeable and soluble vimentin during hormone-induced melanosome movement than in steady state cells. (A) GFP-vimentin-expressing *Xenopus* melanophores (stable cell line) were imaged before and during recovery after photobleaching. The fluorescence recovery of cells (treated with α-MSH) during active melanosome dispersion and post-dispersion was compared. Contrast was adjusted in the 1000 second frame to visually normalize for overall loss of fluorescence during imaging. Scale bars: 10 µm. (B) Quantitative analysis of fluorescence recovery after photobleaching, both during (blue) and after (pink) melanosome dispersion. The result suggests a higher fraction of exchangeable vimentin during melanosome dispersion. The values are averages from four cells under each condition. The difference between the average $t_{1/2}$s between dispersing and fully dispersed cells was statistically significant (P=0.037). Error bars indicate the standard deviation. (C) Western blot analysis shows a transient increase in vimentin solubility in response to melatonin (+MEL) or α-MSH (+MSH) treatment, followed by a decrease to initial levels. Soluble (sup) and pelletable fractions (pellet) from IF-enriched preparations were separated by centrifugation at 12,000 ***g*** for 10 minutes (see Materials and Methods). (D) Changes in the percentage of soluble vimentin in response to hormone treatment were quantified from western blots. Averages from three experiments for each treatment are shown (blue, α-MSH; orange, melatonin). The increase in solubility from time 0 to 40 minutes after treatment with melatonin was statistically significant (P=0.02). Similarly, changes in solubility between 0 and 30 minutes after treatment with α-MSH were also statistically significant (P=0.0072). The decrease in solubility between 40 or 30 minutes and 60 minutes after treatment was also significant for both treatments (P=0.018 for melatonin and 0.026 for α-MSH). Error bars indicate the standard deviation.

for 3 hours and then treated with hormones for 20 minutes and then lysed. However, quantitative analysis of vimentin immunoprecipitated from hormone-treated and control cell lysates showed no significant changes in phosphorylation levels (unpublished data).

Remodeling of the vimentin IF network during melanosome dispersion

Live-imaging of the GFP-vimentin IF network in α-MSH-treated cells not only showed highly dynamic and flexible filaments, but also an overall remodeling of the network. In many of the aggregated cells, most of the vimentin network was concentrated around a perinuclear aggregate of melanosomes. However, as the granules dispersed, the IF network became more evenly distributed between the perinuclear and peripheral cytoplasm (Fig. 8; supplementary material Movie 3). The movement of IFs into the periphery was coincident with the appearance of pigment granules in these regions. These peripheral IFs also appeared to assemble into a more intricate network, consisting of interconnected cage-like structures that surrounded and captured the moving granules. This assembly could also be the result of the de novo formation of IFs and not simply a reorganization of existing IFs. This construction of a filamentous network in the peripheral cytoplasm appeared to be temporally related to the decline in vimentin solubility upon the completion of the dispersion process described above (Fig. 7D).

Discussion

Our results suggest that vimentin IFs may regulate melanosome movement through a physical association. The association can be seen both microscopically in the form of cage-like structures of IFs closely surrounding individual melanosomes, and biochemically as demonstrated by co-purification through Percoll gradients. Remarkably, this interaction appears to be specific for melanosomes. Lysosomes, which are closely related organelles that share many steps of the melanosome biogenesis pathway (Raposo et al., 2007), do not display such intricate associations with vimentin IFs, nor are their movements affected by the disruption of the IF network. Live-cell imaging demonstrates that the association between vimentin and melanosomes is highly dynamic with vimentin IFs constantly changing shape and undergoing extensive distortions during rapid melanosome movement. This distortion most probably reflects a ‘softening of the filaments’ in response to α-MSH treatment, which permits the melanosomes to move more persistently as the IFs become more flexible. This is supported by a significant increase in vimentin solubility and in the exchangeable subunit pool detected during active dispersion and aggregation. The increased distortion could also be related to disruption of IF-melanosome interactions, further enhancing their motility. Near the completion of organelle dispersion, vimentin IFs becomes less soluble and they again form cage-like structures which appear to capture incoming granules.

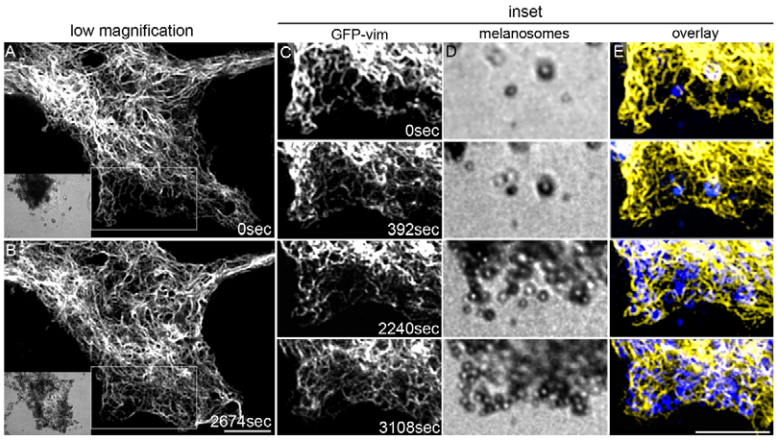

Fig. 8. Vimentin IF network remodeling in response to α-MSH. Time-lapse frames (from Movie 3 in supplementary material) show GFP-vimentin networks re-distributing towards the periphery of the cell (A and B; granules are shown in lower left insets). Higher magnification images show vimentin filaments forming a cage-like network in the peripheral cytoplasm as granules move in to the region (C-E; vimentin is shown in yellow and granules in blue in E; compare vimentin distributions between first and last time frames). Scale bars: 5 μm. Vimentin IF network dynamics during aggregation of granules can also be seen in Movie 2 in supplementary material.

Determination of the exact mechanism of interaction between IFs and melanosomes will require future investigations. However, some interesting clues can be obtained from existing literature. For example, similar roles for IFs in regulating the distribution of membrane-bound organelles have been proposed in late endosome/lysosome positioning, specifically through interactions between IFs and AP3. AP3 is a clathrin adaptor complex also responsible for protein targeting to melanosomes (Styers et al., 2004; Kantheti et al., 1998). Interestingly, we did not observe a difference in the movement of lysosomes between melanophores expressing wild-type vimentin and dominant-negative vimentin. The apparent specificity in the interaction between vimentin and melanosomes in melanophores suggests that AP3 might not play a direct role in this interaction.

Mitochondria have also been shown to be associated with neurofilaments (NFs). Neurofilaments are type IV IFs, composed of the neurofilament triplet proteins, NFL, NFM and NFH (Hoffman and Lasek, 1975; Liem et al., 1978; Schlaepfer and Freeman, 1978). Both NFM and NFH have long non-α-helical C-terminal domains that has been shown to form bridges to mitochondria in electron microscope observations of frog axons (Hirokawa, 1982). The interaction between NFs and mitochondria appears to be regulated by the phosphorylation state of the C-terminal domains of NFH and the membrane potential of mitochondria (Wagner et al., 2003). The kinase-phosphatase equilibrium, which has been shown to regulate the phosphorylation state of IF proteins (Eriksson et al., 2004), could be an efficient mechanism for regulating this interaction and in turn be responsible for the positioning of mitochondria in the cytoplasm.

Kinase-phosphatase equilibria have also been shown to regulate solubility or the assembly state of IFs (reviewed by Chou et al., 2007). In our study, we observed increased solubility of vimentin during active melanosome movement in response to melatonin and α-MSH. This change in solubility does not seem to be a result of changes in total vimentin phosphorylation levels. However, vimentin phosphorylation at certain sites that regulate solubility may be accompanied by de-phosphorylation at other sites, resulting in no net change in total phosphorylation levels. This is an attractive hypothesis given that melatonin and α-MSH are known to induce granule movement by triggering changes in intracellular cAMP and protein kinase A (PKA) activity (reviewed by Sugden et al., 2004). In support of this, PKA has been shown to phosphorylate vimentin, both in vitro and in vivo, driving depolymerization and reorganization of the IF network (Lamb et al., 1989; Eriksson et al., 2004).

The increased fluorescence recovery rates and solubility of vimentin during granule movement may reflect a change in the mechanical properties of the cage-like IF structures surrounding the melanosomes, allowing their translocation through the cytoplasm. However, the solubilized vimentin could also be involved in various signaling processes or even in the regulation of molecular motors. In a report by Perlson et al. (Perlson et al., 2005), axonal injury induced the local translation of a soluble form of vimentin, which served as an adaptor between dynein and phosphorylated ERK (extracellular signal-regulated kinase) to facilitate the transport of the latter from the injured axon to the cell nucleus. The direct binding to vimentin also protected the phosphorylated ERK from phosphatases (Perlson et al., 2006). Interestingly, ERK signaling has also been implicated in the regulation of melanosome transport. Inhibition of ERK signaling by the MEK (MAPK/ERK kinase) inhibitor U0126 blocks bi-directional melanosome transport along MTs whereas constitutively active MEK1/2 stimulates transport (Deacon et al., 2005). These changes in transport appear to be unbiased, affecting movement in both directions, which is similar to the global increase in melanosome movements seen in cells with disrupted vimentin IF networks (Kural et al., 2007). Interestingly, both ERK and MEK have been found in purified melanosome fractions and appear to be transiently phosphorylated upon stimulation of cells with hormones (Deacon et al., 2005). Vimentin could potentially behave as a scaffold or a local sink for MAP kinases such as ERK and perhaps even regulate their activity, which in turn could regulate motor activity on the melanosomes.

Alternatively, as one of the major cargoes for molecular motors (Helfand et al., 2002), vimentin IFs could regulate melanosome motility by directly competing for motor binding. The dynactin complex, typically known as the cargo adaptor for cytoplasmic dynein, has also been shown to interact directly with kinesin II components and has been implicated in the coordination of dynein and kinesin activities in melanosome transport (Deacon et al., 2003). Dynactin has been shown to contain a common binding site for both motors and when the availability of this binding site is inhibited, transport in both directions is impeded (Deacon et al., 2003). Similarly, vimentin could impede melanosome motility through competitive binding with the motors.

Although motility assays show that IFs impede granule movement, the end-states at 60 minutes after dispersion or aggregation does not appear to be different between cells that contain intact IF networks and those that do not. So the question arises as to what other role(s) IFs may play during granule

movement? There are several possibilities. An early study by Porter and McNiven (Porter and McNiven, 1982) showed that individual pigment granules in squirrel fish erythrophores always returned to the same position in the cytoplasm during multiple cycles of dispersion. Why the cell would need such precise positioning (as opposed to a random distribution of granules) is unclear. However, the movies showing vimentin IFs surrounding and capturing incoming melanosomes near the completion of dispersion suggest that the IF network may be a good candidate for the targeted positioning of melanosomes. Another possibility is in the coordination of melanosome movement. The highly interconnected, honeycomb-like structure of the IF network provides a mechanism for transmitting information between and amongst moving melanosomes. For example, the movement of one melanosome, which bends and distorts the IFs surrounding it, could in turn, affect the structure of the entire IF network and the neighboring melanosomes encaged within it, effectually transforming individual melanosomes into a melanosome network. The coordination of melanosome movements, mediated by the surrounding IF network, may enhance the efficiency of mass movement and may perhaps allow for faster reversals between mass aggregation and dispersion. Somewhat analogous to a fishing net, one could imagine that mass movements of melanosomes would be easier to stop and reverse in a global manner if individual melanosomes were enmeshed in a network. This ability could in turn, provide a physiological advantage for the organism. It is interesting to note that early studies of fish pigment cells described the existence of a 'microtrabecular' filament lattice, which mediated the association between granules and microtubules (Byers and Porter, 1977). Based on electron micrographs of these cells following the extraction of MTs and MFs it was suggested that IFs are a component of this lattice (Murphy and Grasser, 1984).

Surprisingly, the vimentin IF system in melanophores is not affected by microtubule depolymerization. This is in contrast to the literature describing the intimate relationship between vimentin IFs and MTs, mediated by cross-bridging proteins such as plectin and molecular motors (reviewed by Helfand et al., 2004). This apparent autonomy of IFs distribution is not explained by their attachments to melanosomes, as it is observed not only in normal melanophores, but also in melanophores treated with PTU that contain no melanosomes. However, the literature also describes interactions between vimentin and the actin cytoskeleton. In particular, Hollenbeck et al. (Hollenbeck et al., 1989) have shown that the retraction of vimentin IFs towards the perinuclear region in response to microtubule-depolymerizing drugs is dependent on ATP and the actin cytoskeleton, suggesting a balance in interactions between all three cytoskeletal systems. Furthermore, it is possible that, in melanophores, vimentin IFs interact more readily with the actin cytoskeleton than with MTs, akin to type I and II keratin IFs (Yoon et al., 2001; Windoffer et al., 2006). Future studies will be needed to address the interactions between IFs and the actin network in melanosome movement.

Either directly or indirectly through interactions with adaptors such as AP3, MAP kinases and/or microtubule- and actin-associated motors, vimentin IFs could increase the number of pauses and reversals during melanosome movement, thereby decreasing their run-lengths and regulating their motility. It is also intriguing to speculate that the honeycomb-like structure of the IF network might increase the coordination of melanosome movements, potentially allowing the melanophore to quickly respond to changing stimuli.

In conclusion, it is apparent that the transport and positioning of melanosomes requires the coordinated regulation of IFs along with the other cytoskeletal systems.

Materials and Methods

Cell culture

Immortalized *Xenopus laevis* melanophores were cultured as described previously (Rogers et al., 1997). For aggregation and dispersion experiments, cells were serum starved for 2 hours in the dark before the addition of 10 nM melatonin or 100 nM α-MSH. A melanophore line stably expressing GFP-vimentin was established by transfecting cells with a plasmid encoding GFP-vimentin fusion proteins (see below) and selecting stably transfected cells with G-418. Melanosome-free cells were generated by maintaining melanophores in culture medium supplemented with 1 mM 1-phenyl 2-thiourea (PTU), for at least 3 weeks (Gross et al., 2002). For transfection experiments, cells were transfected using Fugene 6 (Roche Diagnostics, Indianapolis, IN), 48 hours before experimentation and analysis.

Indirect Immunofluorescence

Melanophores cultured on poly-L-lysine-coated coverslips were fixed with 3.7% formaldehyde followed by detergent extraction with 0.05% Triton X-100. A rabbit antibody raised against hamster vimentin (#264) was used for the detection of *Xenopus* vimentin. This antibody recognizes a single vimentin band in *Xenopus* melanophore lysates. For tubulin detection, a monoclonal antibody DM1α was used. Alexa-Fluor-conjugated phalloidin was used for the detection of actin filaments. In all preparations, Alexa-Fluor-conjugated secondary antibodies (goat; Molecular Probes) were used. Cells were then imaged on a Zeiss LSM 510 scanning confocal microscope, with a 100×, 1.45 NA objective (Carl Zeiss). Bright-field illumination was used to image melanosomes.

Lysosomal staining

For microscopic analysis of the distribution of lysosomes and vimentin IFs, melanophores were incubated in medium supplemented with LysoTracker Red DND-99 (Invitrogen Corp., Carlsbad, CA) for 1 hour, according to the manufacturer's guidelines, and then rinsed twice with fresh medium followed by fixation and immunofluorescence preparation for detection of vimentin. For lysosomal tracking analyses, melanosome-free melanophores were transfected with either GFP-vimentin or GFP-vimentin(1-138) and incubated with LysoTracker Red DND-99 for 30 minutes and then rinsed twice with fresh medium.

Platinum replica electron microscopy

For MT-free IF-enriched cytoskeletal preparations, cells were extracted in PEM (100 mM PIPES pH 6.9, 1 mM EGTA, 1 mM $MgCl_2$) buffer with 1% Triton X-100, 0.4 M NaCl and 1 mg/ml DNase I for 10 minutes. To remove any residual actin, all preparations were treated with gelsolin (purified from human plasma; Cytoskeleton). Cells were then fixed with 2% glutaraldehyde and stained with 0.1% tannic acid and 0.2% uranyl acetate. These preparations were then processed by critical point drying followed by rotary shadowing with platinum and carbon (Svitkina et al., 1995). Ultrastructural observations of cytoskeletal preparations were performed as described elsewhere (Svitkina et al., 1995).

Melansome purification

Isolation of melanosomes from melanophores was carried out as described by Rogers et al. (Rogers et al., 1997).

DNA construct preparation

The full-length *Xenopus* GFP-vimentin was a gift from Harald Herrmann (German Cancer Research Center (DKFZ), Heidelberg, Germany); the cDNA of *Xenopus laevis* vimentin 1 (accession no. BC085223) was cloned into a pEGFP-C1 vector using BspE1 restriction sites on both 5′ and 3′ ends. The dominant negative construct, GFP-vimentin(1-138), was constructed by cloning the cDNA corresponding to the first 138 amino acids of the hamster vimentin into a pEGFP-N1 vector between *Eco*RI and *Bam*HI sites. This vimentin fragment consists of the non-α-helical head domain (residues 1-102) and the highly conserved α-helical domain (1A region).

Quantitative analysis of organelle movement

Cells were incubated in serum-free medium for 2 hours and stimulated with melatonin or α-MSH as described. Time-lapse movies were recorded for 1 minute, 15 minutes after stimulation. Images were acquired every 1 second, using a Nikon U-2000 microscope, with the CoolSnap CCD camera (Photometrics; for melanosome imaging) or a Cascade II EMCCD camera (Photometrics; for fluorescent lysosome imaging), both driven by Metamorph software (Molecular Devices). Bright-field illumination filtered below 695 nm was used for imaging melanosomes to avoid activation of melanopsin. Organelle movements were tracked using Diatrack 3.0 (Semasopht, Chavannes-près-Renens, Switzerland) and the tracks were split into trajectories directed to and from the cell center. Vectors lengths (displacements of particles between two consecutive frames) were exported into Microsoft Excel.

Live imaging and fluorescence recovery after photobleaching (FRAP)

Melanophores stably expressing GFP-vimentin were cultured on poly-L-lysine coated Lab-tek chambered coverglasses (VWR, West Chester, PA). Cells were serum-starved for 2 hours before imaging, during which 100 nM α-MSH was added to induce melanosome dispersion. In some instances, H-89 (40 μM) was used to image melanosome aggregation. For high resolution live imaging, cells were imaged on a Yokogawa spinning disc confocal microscope (Nikon) with a ×100, 1.45NA, Nikon objective. Images were captured every 5-10 seconds with 30-100 msecond exposure times using a Hamamatsu electron multiplier CCD digital camera. FRAP experiments were carried out on a Zeiss LSM 510 scanning confocal microscope, with a ×100, 1.45NA, Zeiss objective (Carl Zeiss). A 2-4 μm wide line was bleached along a melanophore and the recovery was imaged every 10 seconds. For each time point after the photobleaching event, the mean intensity of the photobleached region was normalized to the mean intensity prior to photobleaching. The mean intensity of a similar sized region in another part of the cell that was not photobleached was used to compensate for photobleaching that occurred during the time-lapse imaging of the recovery period. Final intensity values were adjusted in order to display the value at the first time point following photobleaching as zero. Cells were analyzed by FRAP during melanosome movement in α-MSH (n=4 cells; only cells in which the melanosomes were fully aggregated before hormone addition were used) and at the end of dispersion (n=4 cells). $t_{1/2}$ values were calculated for each experiment based on a fitted logarithmic curve. The differences in $t_{1/2}$ between cells undergoing dispersion and in fully dispersed cells were tested for statistical significance using t-tests.

Vimentin solubility assay

Melanophores cultured in 60 mm dishes were serum starved for 2 hours and then treated with melatonin (10 nM) or α-MSH (100 nM) for various durations in the dark. Cells were collected every 10 minutes and lysed in high salt, detergent buffer [400 μl/dish; 20 mM Tris-HCl, pH 7.4, 600 mM NaCl, 2 mM EDTA, 2 mM EGTA, 50 nM calyculin A, 0.5% Triton X-100 and protease inhibitors (Roche)]. The soluble and pelletable (IF enriched) fractions were separated by centrifugation at 12,000 ***g*** for 10 minutes. After centrifugation, SDS sample buffer was added to soluble and pelletable fractions, bringing the volume of both samples to the same level and then heated. The relative distribution of vimentin between soluble and pelletable fractions was measured by quantitative western blotting using purified GFP-human-vimentin as a standard and a Kodak Image Station 440. Three independent experiments were carried out for each hormone treatment and the statistical significance of the differences seen in soluble fractions between 0 minutes and 30-40 minutes and between 30-40 minutes and 60 minutes were analyzed using t-tests.

^{32}P labeling

Cells cultured in 100 mm dishes (in the dark) were preloaded with 250 μCi ^{32}P/dish for 2 hours in 10 ml of 0.7× phosphate-free DMEM (Gibco 11971) plus 5% dialyzed calf serum. The medium was then replaced with fresh ^{32}P medium without serum for one more hour. α-MSH or melatonin was added in the last 20 minutes of incubation. Each dish of cells was lysed in 1 ml of the following buffer: 20 mM Tris-HCl (pH 7.4), 150 mM NaCl, 2 mM EDTA, 2 mM EGTA, 40 nM calyculin A, 0.2% SDS and protease inhibitors. Lysates were immediately heated for 10 minutes and then cooled on the bench and centrifuged for 10 minutes at 12,000 ***g***. Triton X-100 (2%) was added to the supernatants and vimentin was immuno-absorbed with 50 μl of vimentin-specific rabbit serum 264 and 30 μl of protein A beads (Sigma). The absorbed proteins were rinsed three times with PBS containing 0.1% Triton X-100 and fixed in SDS gel sample buffer for analysis. Radioactivity of ^{32}P was quantified using the Cyclone Phosphor Image System (Perkin Elmer).

This work was supported by NIGMS (NIH) grants to V.I.G. (GN-52111) and R.D.G. (GM-38606). Deposited in PMC for release after 12 months.

References

Byers, H. R. and Porter, K. R. (1977). Transformations in the structure of the cytoplasmic ground substance in erythrophores during pigment aggregation and dispersion: A study using whole-cell preparations in stereo high voltage electron microscopy. *J. Cell Biol.* **75**, 541-558.

Chang, L. and Goldman, R. D. (2004). Intermediate filaments mediate cytoskeletal crosstalk. *Nat. Rev. Mol. Cell Biol.* **5**, 601-613.

Chijiwa, T., Mishima, A., Hagiwara, M., Sano, M., Hayashi, K., Inoue, T., Naito, K., Toshioka, T. and Hidaka, H. (1990). Inhibition of forskolin-induced neurite outgrowth and protein phosphorylation by a newly synthesized selective inhibitor of cyclic AMP-dependent protein kinase, N-[2-(p-bromocinnamylamino)ethyl]-5-isoquinolinesulfonamide (H-89), of PC12D pheochromocytoma cells. *J. Biol. Chem.* **265**, 5267-5272.

Chou, Y. H., Flitney, F. W., Chang, L., Mendez, M., Grin, B. and Goldman, R. D. (2007). The motility and dynamic properties of intermediate filaments and their constituent proteins. *Exp. Cell Res.* **313**, 2236-2243.

Collier, N. C., Sheetz, M. P. and Schlesinger, M. J. (1993). Concomitant changes in mitochondria and intermediate filaments during heat shock and recovery of chicken embryo fibroblasts. *J. Cell Biochem.* **52**, 297-307.

Daniolos, A., Lerner, A. B. and Lerner, M. R. (1990). Action of light on frog pigment cells in culture. *Pigment Cell Res.* **3**, 38-43.

Deacon, S. W., Serpinskaya, A. S., Vaughan, P. S., Lopez Fanarraga, M., Vernos, I., Vaughan, K. T. and Gelfand, V. I. (2003). Dynactin is required for bidirectional organelle transport. *J. Cell Biol.* **160**, 297-301.

Deacon, S. W., Nascimento, A., Serpinskaya, A. S. and Gelfand, V. I. (2005). Regulation of bidirectional melanosome transport by organelle bound MAP kinase. *Curr. Biol.* **15**, 459-463.

Eriksson, J. E., He, T., Trejo-Skalli, A. V., Härmälä-Braskén, A. S., Hellman, J., Chou, Y. H. and Goldman, R. D. (2004). Specific in vivo phosphorylation sites determine the assembly dynamics of vimentin intermediate filaments. *J. Cell Sci.* **117**, 919-932.

Gao, Y. and Sztul, E. (2001). A novel interaction of the Golgi complex with the vimentin intermediate filament cytoskeleton. *J. Cell Biol.* **152**, 877-894.

Gao, Y. S., Vrielink, A., MacKenzie, R. and Sztul, E. (2002). A novel type of regulation of the vimentin intermediate filament cytoskeleton by a Golgi protein. *Eur. J. Cell Biol.* **81**, 391-401.

Goldman, R. D. (1971). The role of three cytoplasmic fibers in BHK-21 cell motility. I. Microtubules and the effects of colchicine. *J. Cell Biol.* **51**, 752-762.

Goldman, R. D., Khuon, S., Chou, Y. H., Opal, P. and Steinert, P. M. (1996). The function of intermediate filaments in cell shape and cytoskeletal integrity. *J. Cell Biol.* **134**, 971-983.

Gross, S. P., Tuma, M. C., Deacon, S. W., Serpinskaya, A. S., Reilein, A. R. and Gelfand, V. I. (2002). Interactions and regulation of molecular motors in Xenopus melanophores. *J. Cell Biol.* **156**, 855-865.

Gyoeva, F. K., Leonova, E. V., Rodionov, V. I. and Gelfand, V. I. (1987). Vimentin intermediate filaments in fish melanophores. *J. Cell Sci.* **88**, 649-655.

Helfand, B. T., Mikami, A., Vallee, R. B. and Goldman, R. D. (2002). A requirement for cytoplasmic dynein and dynactin in intermediate filament network assembly and organization. *J. Cell Biol.* **157**, 795-806.

Helfand, B. T., Chang, L. and Goldman, R. D. (2004). Intermediate filaments are dynamic and motile elements of cellular architecture. *J. Cell. Sci.* **117**, 133-141.

Helmke, B. P., Goldman, R. D. and Davies, P. F. (2000). Rapid displacement of vimentin intermediate filaments in living endothelial cells exposed to flow. *Circ. Res.* **86**, 745-752.

Helmke, B. P., Thakker, D. B., Goldman, R. D. and Davies, P. F. (2001). Spatiotemporal analysis of flow-induced intermediate filament displacement in living endothelial cells. *Biophys. J.* **80**, 184-194.

Hirokawa, N. (1982). Cross-linker system between neurofilaments, microtubules, and membranous organelles in frog axons revealed by the quick-freeze, deep-etching method. *J. Cell Biol.* **94**, 129-142.

Hoffman, P. N. and Lasek, R. J. (1975). The slow component of axonal transport. Identification of major structural polypeptides of the axon and their generality among mammalian neurons. *J. Cell Biol.* **66**, 351-366.

Hollenbeck, P. J., Bershadsky, A. D., Pletjushkina, O. Y., Tint, I. S. and Vasiliev, J. M. (1989). Intermediate filament collapse is an ATP-dependent and actin-dependent process. *J. Cell Sci.* **92**, 621-631.

Janmey, P. A., Shah, J. V., Janssen, K. P. and Schliwa, M. (1998). Viscoelasticity of intermediate filament networks. *Subcell. Biochem.* **31**, 381-397.

Kantheti, P., Qiao, X., Diaz, M. E., Peden, A. A., Meyer, G. E., Carskadon, S. L., Kapfhamer, D., Sufalko, D., Robinson, M. S., Noebels, J. L. et al. (1998). Mutation in AP-3 delta in the mocha mouse links endosomal transport to storage deficiency in platelets, melanosomes, and synaptic vesicles. *Neuron* **21**, 111-122.

Kreplak, L., Bär, H., Leterrier, J. F., Herrmann, H. and Aebi, U. (2005). Exploring the mechanical behavior of single intermediate filaments. *J. Mol. Biol.* **354**, 569-577.

Kural, C., Serpinskaya, A. S., Chou, Y. H., Goldman, R. D., Gelfand, V. I. and Selvin, P. R. (2007). Tracking melanosomes inside a cell to study molecular motors and their interaction. *Proc. Natl. Acad. Sci. USA* **104**, 5378-5382.

Lamb, N. J., Fernandez, A., Feramisco, J. R. and Welch, W. J. (1989). Modulation of vimentin containing intermediate filament distribution and phosphorylation in living fibroblasts by the cAMP-dependent protein kinase. *J. Cell Biol.* **108**, 2409-2422.

Liem, R. K., Yen, S. H., Salomon, G. D. and Shelanski, M. L. (1978). Intermediate filaments in nervous tissues. *J. Cell Biol.* **79**, 637-645.

Mose-Larsen, P., Bravo, R., Fey, S. J., Small, J. V. and Celis, J. E. (1982). Putative association of mitochondria with a subpopulation of intermediate-sized filaments in cultured human skin fibroblasts. *Cell* **31**, 681-692.

Murphy, D. B. and Grasser, W. A. (1984). Intermediate filaments in the cytoskeletons of fish chromatophores. *J. Cell Sci.* **66**, 353-366.

Perlson, E., Hanz, S., Ben-Yaakov, K., Segal-Ruder, Y., Seger, R. and Fainzilber, M. (2005). Vimentin-dependent spatial translocation of an activated MAP kinase in injured nerve. *Neuron* **45**, 715-726.

Perlson, E., Michaelevski, I., Kowalsman, N., Ben-Yaakov, K., Shaked, M., Seger, R., Eisenstein, M. and Fainzilber, M. (2006). Vimentin binding to phosphorylated Erk sterically hinders enzymatic dephosphorylation of the kinase. *J. Mol. Biol.* **364**, 938-944.

Porter, K. R. and McNiven, M. A. (1982). The cytoplast: a unit structure in chromatophores. *Cell* **29**, 23-32.

Provencio, I., Jiang, G., De Grip, W. J., Hayes, W. P. and Rollag, M. D. (1998). Melanopsin: an opsin in melanophores, brain, and eye. *Proc. Natl. Acad. Sci. USA* **95**, 340-345.

Rao, M. V., Engle, L. J., Mohan, P. S., Yuan, A., Qiu, D., Cataldo, A., Hassinger, L., Jacobsen, S., Lee, V. M., Andreadis, A. et al. (2002). Myosin Va binding to

neurofilaments is essential for correct myosin Va distribution and transport and neurofilament density. *J. Cell Biol*. **159**, 279-290.

Raposo, G., Marks, M. S. and Cutler, D. R. (2007). Lysosome-related organelles: driving post-Golgi compartments into specialization. *Curr. Opin. Cell Biol.* **19**, 394-401.

Rogers, S. L. and Gelfand, V. I. (1996). Myosin cooperates with microtubule motors during organelle transport in melanophores. *Curr. Biol*. **8**, 161-164.

Rogers, S. L., Tint, I. S., Fanapour, P. C. and Gelfand, V. I. (1997). Regulated bidirectional motility of melanophore pigment granules along microtubules in vitro. *Proc. Natl. Acad. Sci. USA* **94**, 3720-3725.

Schlaepfer, W. W. and Freeman, L. A. (1978). Neurofilament proteins of rat peripheral nerve and spinal cord. *J. Cell Biol*. **78**, 653-662.

Sivaramakrishnan, S., DeGiulio, J. V., Lorand, L., Goldman, R. D. and Ridge, K. M. (2008). Micromechanical properties of keratin intermediate filament networks. *Proc. Natl. Acad. Sci. USA* **105**, 889-894.

Styers, M. L., Salazar, G., Love, R., Peden, A. A., Kowalczyk, A. P. and Faundez, V. (2004). The endo-lysosomal sorting machinery interacts with the intermediate filament cytoskeleton. *Mol. Biol. Cell* **15**, 5369-5382.

Styers, M. L., Kowalczyk, A. P. and Faundez, V. (2005). Intermediate filaments and vesicular membrane traffic: the odd couple's first dance? *Traffic* **6**, 359-365.

Sugden, D., Davidson, K., Hough, K. A. and The, M. T. (2004). Melatonin, melatonin receptors and melanophores: a moving story. *Pigment Cell Res*. **17**, 454-460.

Svitkina, T. M., Verkhovsky, A. B. and Borisy, G. G. (1995). Improved procedures for electron microscopic visualization of the cytoskeleton of cultured cells. *J. Struct. Biol*. **115**, 290-303.

Wagner, O. I., Lifshitz, J., Janmey, P. A., Linden, M., McIntosh, T. K. and Leterrier, J. F. (2003). Mechanisms of mitochondria-neurofilament interactions. *J. Neurosci*. **23**, 9046-9058.

Windoffer, R., Kölsch, A., Wöll, S. and Leube, R. E. (2006). Focal adhesions are hotspots for keratin filament precursor formation. *J. Cell Biol*. **173**, 341-348.

Yoon, K. H., Yoon, M., Moir, R. D., Khuon, S., Flitney, F. W. and Goldman, R. D. (2001). Insights into the dynamic properties of keratin intermediate filaments in living epithelial cells. *J. Cell Biol*. **153**, 503-516.

Zimek, A., Stick, R. and Weber, K. (2003). Genes coding for intermediate filament proteins: common features and unexpected differences in the genomes of humans and the teleost fish Fugu rubripes. *J. Cell Sci*. **116**, 2295-2302.